Coupling of orthogonally polarized waves and vectorial coherent oscillation in periodically poled $LiNbO_3$:Y:Fe

D. Barilov and A. Shumelyuk

Institute of Physics, National Academy of Sciences, 03650, Kiev-39, Ukraine

L. Hesselink

Stanford University, Room 353 Durand Building, Stanford, California 94305-4035

B. Sturman

International Institute for Nonlinear Studies, Koptyug Avenue 1, 630090, Novosibirsk, Russia

S. Odoulov

Institute of Physics, National Academy of Sciences, 03650, Kiev-39, Ukraine

Received November 9, 2002; revised manuscript received March 31, 2003

Photorefractive grating recording with two orthogonally polarized eigenwaves (ordinary and extraordinary) and vectorial coherent oscillation in a backward four-wave mixing scheme in iron-doped periodically poled lithium niobate are reported. © 2003 Optical Society of America

OCIS codes: 190.4720, 210.4810, 090.2900, 090.7330.

1. INTRODUCTION

Periodically poled ferroelectric crystals are known as promising materials for quasi-phase-matched frequency conversion owing to their $\chi^{(2)}$ nonlinearity.[1–3] At low intensities, these artificially tailored materials also exhibit strong photorefractive nonlinearity.[4] It has been shown that iron-doped periodically poled lithium niobate (PPLN) has the same sensitivity to holographic grating recording as homogeneously poled material but exhibits an inhibited response at low spatial frequencies; i.e., this material is optical-damage free.[5,6]

Efficient recording of Bragg-matched three-dimensional index gratings is possible in PPLN:Fe because of the photovoltaic charge transport.[7] The nonlinear change of optical permittivity $\Delta\epsilon$ is proportional in this case to the product of an effective photovoltaic constant β_{eff} and an effective electro-optic constant r_{eff}. Both β_{eff} and r_{eff} are sensitive to inversion of the crystal polar axis; they change sign in each new domain of the opposite spontaneous polarization. The sign of the product $\beta_{\text{eff}}r_{\text{eff}}$ remains, however, the same throughout the whole layered structure; this ensures continuity of the recorded phase grating and facilitates attaining high diffraction efficiency.

Until now, efficient recording of index gratings was achieved in PPLN by use of longitudinal photovoltaic currents,[5] i.e., currents that propagate along the optical z axis and are proportional to the diagonal components of the photovoltaic tensor. Charge separation occurs in this case owing to the spatial intensity modulation produced by either ordinary or extraordinary light waves.

It is known, however, that the photovoltaic tensor possesses nondiagonal components in lithium niobate ($LiNbO_3$); the corresponding photovoltaic currents can be excited only when ordinary and extraordinary light waves are present simultaneously in the sample.[7] This fact has allowed for pure polarization recording (in the absence of spatial modulation of the light intensity) of the index grating in single-domain $LiNbO_3$:Fe crystals.[8]

In this paper we prove the possibility of such polarization grating recording in PPLN:Y:Fe. The feasibility of polarization recording in the single-domain case does not guarantee its feasibility in PPLN because a large amount of yttrium is deliberately introduced into the melt to stabilize the final domain structure.[9]

We report (i) efficient polarization recording of index gratings with high spatial frequencies and inhibited optical damage, (ii) strong intensity redistribution for the corresponding orthogonally polarized recording waves (vectorial coupling), (iii) efficient generation of phase-conjugate waves in a backward four-wave mixing geometry, and (iv) coherent high-quality oscillation in a cavity formed by conventional and phase-conjugate mirrors. Finally, using the experimental data, we evaluate the effective photovoltaic field that characterizes the polarization recording.

0740-3224/2003/081649-07$15.00

2. PHYSICAL BACKGROUND

Photorefractive nonlinearity is caused by a light-induced charge separation leading to spatial variations of the optical permittivity tensor $\delta\hat{\epsilon}$ owing to the linear electro-optic effect. For the Cartesian components of the permittivity tensor one can write

$$\delta\epsilon_{mn}(\mathbf{r}) \simeq -n^4 r_{mnl} E_l(\mathbf{r}), \tag{1}$$

where $n = (n_o + n_e)/2 \simeq n_{o,e}$ is the average refractive index, n_o and n_e are refractive indices for ordinary and extraordinary waves, respectively, r_{mnl} is an electro-optic tensor, and E_l is the lth component of the space-charge field. The largest components of the electro-optic tensor are $r_{333} \equiv r_{33}$, $r_{113} \equiv r_{13}$, and $r_{131} \equiv r_{51}$. Components r_{33} and r_{13} are responsible for coupling between waves of the same polarization, extraordinary (e) and ordinary (o), respectively, whereas component r_{51} is responsible for the mutual coupling of o and e waves.

In PPLN:Fe, the light-induced charge transport is predominantly due to the bulk photovoltaic effect.[7] The mth component of photovoltaic current density $\mathbf{j}$ is

$$j_m = \beta_{mnl} A_n A_l^*, \tag{2}$$

where β_{mnl} is the photovoltaic tensor and $\mathbf{A}$ is the complex slowly varying (in time) amplitude of the electric light-field vector such that $I = |\mathbf{A}|^2$ is the light intensity.

The photovoltaic tensor is generally complex; it can be represented in the form[7]

$$\beta_{mnl} = \beta^L_{mnl} + i\,\delta_{mnk}\beta^C_{kl}, \tag{3}$$

where $\hat{\beta}^L$ and $\hat{\beta}^C$ are real tensors that describe the so-called linear and circular photovoltaic currents and δ_{mnk} is the unit antisymmetric tensor. Tensor β^L_{mnl} is symmetric to permutation of subscripts n and l. Its independent components are $\beta^L_{33} \equiv \beta^L_{333}$, $\beta^L_{31} \equiv \beta^L_{311}$, and $\beta^L_{15} \equiv \beta^L_{131}$. Components β^L_{33} and β^L_{31} correspond to the longitudinal currents induced by light polarized parallel and perpendicular, respectively, to the optical axis. Component β^L_{15} is responsible for the current flowing perpendicular to the polar axis; to excite this transverse current, the light field has to possess simultaneously components that are parallel and perpendicular to the z axis. In other words, o and e waves have to be present simultaneously in the crystal. Component β^C_{12} is also responsible for the transverse photovoltaic current induced by o and e waves. Because the wave vectors of these waves are different, the transverse currents are spatially oscillating. The main difference between the transverse spatially oscillating currents related to components β^L_{15} and β^C_{12} is that their distributions are shifted with respect to each other by a quarter of a period. It is known that for iron-doped lithium niobate the inequality $\beta^C_{12} \gg \beta^L_{15}$ holds true.[10]

The photovoltaic currents result in formation of space-charge fields. To describe them it is convenient to introduce the photovoltaic field

$$E^{pv}_m = \beta_{mnl} A_n A_l^*/\sigma, \tag{4}$$

where $\sigma = \kappa I$ is the photoconductivity and κ is the specific photoconductivity.

In accordance with the notation of Eq. (4), we label the photovoltaic fields that are due to the linear photovoltaic currents propagating along the z axis and excited by (e) and (o) waves E^L_{33} and E^L_{31}, respectively. Similarly, fields E^L_{15} and E^C_{12} refer to photovoltaic tensor components β^L_{15} and β^C_{12}. They characterize the result of charge separation caused by the spatially oscillating transverse photovoltaic currents. In $LiNbO_3$ doped with iron or copper longitudinal fields E^L_{33} and E^L_{31} range from a few tens to hundreds of kilovolts per centimeter. Transverse field E^C_{12} in $LiNbO_3$:Fe is roughly 1 order of magnitude smaller than the longitudinal fields and considerably larger than E^L_{15}.

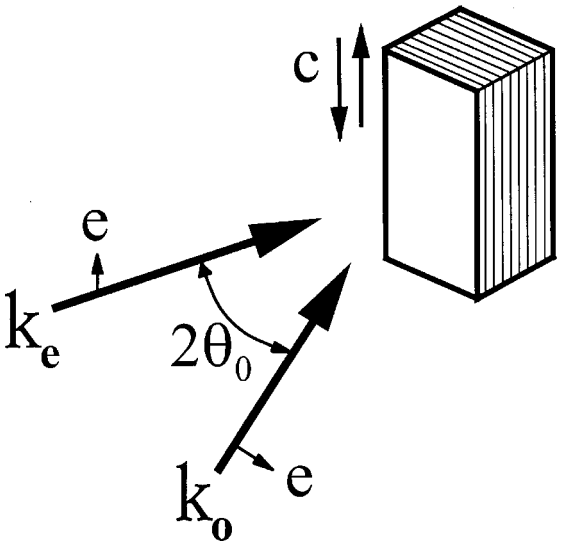

Fig. 1. Schematic representation of photorefractive grating recording with two orthogonally polarized light waves.

The space-charge fields for the gratings recorded in PPLN in different geometries and with different orientations and polarizations of two light beams were calculated in Refs. 4 and 11. For the polarization recording of a grating with grating vector $\mathbf{K}$ perpendicular to the crystal $\mathbf{c}$ axis (see Fig. 1) the amplitude of the fundamental Fourier component of the space-charge field is

$$E^{(0)}_K \approx -iE^C_{12}(\hat{s}\hat{e}_o)^2\left[1 - \frac{2}{Kx_0}\tanh\left(\frac{Kx_0}{2}\right)\right]\frac{A_o A_e^*}{I_0}. \tag{5}$$

Here x_0 is a half-period of the domain structure, $A_{o,e}$ are the scalar amplitudes of ordinary and extraordinary recording waves, $\hat{e}_o$ is the unit polarization vector for the o wave, and $\hat{s} = \mathbf{K}/K$ is the unit grating vector. This expression includes two K-dependent factors; one (in brackets) is due to the periodic poling,[11] and the other,

$$(\hat{s}\hat{e}_o)^2 = \frac{4\theta^2}{4\theta^2 + [(n_o - n_e)/n_o]^2}, \tag{6}$$

is caused by the crystal birefringence.[12] Here θ is the half-angle between the recording beams inside the sample, which is, because of refraction, small enough for $\sin\theta \simeq \theta$ to be considered. Spatial frequency K of the recorded grating is expressed by θ as follows:

$$K = k\{4\theta^2 + [(n_o - n_e)/n_o]^2\}^{1/2}, \tag{7}$$

where $k = 2\pi n_o/\lambda$ is the light wave number. Note that expression (5) also describes the space-charge field in the single-domain case that corresponds to the limit $Kx_0 \to \infty$, i.e., to Eq. (7).

Each of the two K-dependent factors in expression (5) reduces the space-charge field; the smaller the spatial frequency, the stronger the reduction. The cutoff spatial frequency for polarization grating recording (it can be introduced as the frequency for which the amplitude of the space-charge field becomes two times smaller than its maximum value) depends on domain size x_0. This is illustrated in Fig. 2, which shows the spatial frequency dependences for several representative values of the domain sizes, namely, $x_0 = 10, 20, 50$ μm, and also for the single-domain case, $x_0 = \infty$.

To emphasize the role of birefringence for the K dependence of the space-charge field, we have set $n_o = n_e$ in Fig. 2A. This case is relevant also to periodically poled $LiTaO_3$, which possesses only a small birefringence at room temperature. For $LiNbO_3$ the cutoff spatial frequency depends weakly on domain size; see Fig. 2B.

There are several main options for experimental evaluation of the photovoltaic fields. One can measure, e.g., gain factor Γ for two-beam coupling in the geometry of Fig. 1, diffraction efficiency η of the recorded photorefractive grating (Fig. 3A), phase-conjugate reflectivity R_{pc} in the backward four-wave mixing geometry of Fig. 3B, or

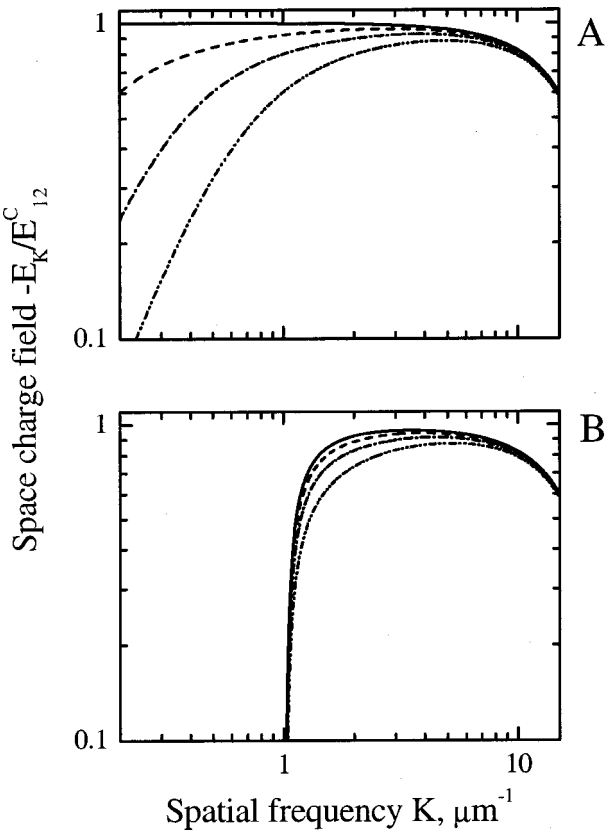

Fig. 2. Calculated space-charge field versus spatial frequency for polarization grating recording. Domain size x_0 is ∞ for the solid curves, 50 μm for dashed curves, 20 μm for dashed–dotted curves and 10 μm for dashed–double-dotted curves. The crystal birefringence $n_o - n_e$ is zero for A and 0.1 for B.

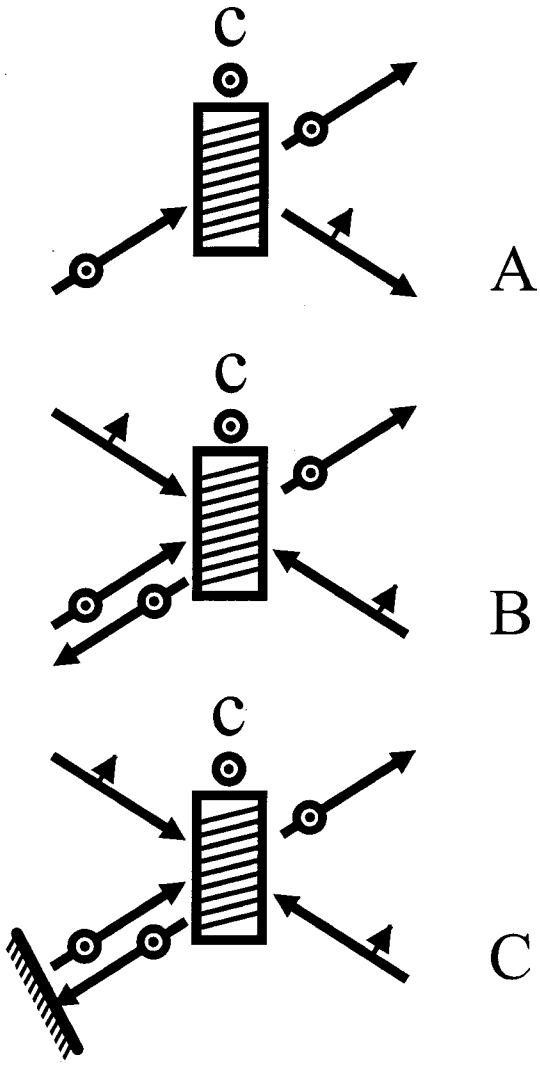

Fig. 3. Schematic representation of measurements of A polarization anisotropic diffraction efficiency, B backward-polarization four-wave mixing, and C, the semilinear coherent oscillator with two counterpropagating ordinary pump beams.

threshold coupling strength $(\Gamma l)_{th}$ for a coherent oscillation (Fig. 3C). The relations that specify the quantities introduced are listed below.

The gain factor for coupling of two orthogonally polarized light waves is[12]

$$\Gamma = \frac{2\pi {n_o}^2 {n_e}^2 r_{51} \beta_{12}^C}{\kappa\lambda \cos\theta} (\hat{s}\hat{e}_o)^2 \left[1 - \frac{2}{Kx_0} \tanh\left(\frac{Kx_0}{2}\right)\right]. \quad (8)$$

The only photovoltaic field entering this expression is $E_{12}^C = \beta_{12}^C/\kappa$.

In the actual case $|E_{15}^L| \ll |E_{12}^C|$, which corresponds to a nonlocal phototefractive response, the expression for the diffraction efficiency is similar to that known for the diffusion nonlinearity[12,13]:

$$\eta = \frac{m}{1 + m} \frac{[\exp(\Gamma l/2) - 1]^2}{[m \exp(\Gamma l) + 1]}, \quad (9)$$

where $m = I_e(0)/I_o(0)$ is the input beam ratio and l is the crystal thickness.

When $|E_{15}^{L}| \ll |E_{12}^{C}|$, the phase-conjugate reflectivity for four-wave mixing with two counterpropagating ordinary pump beams and an *e*-polarized signal beam (Fig. 3B) can be expressed as[14]

$$R_{\mathrm{pc}} = \left(\frac{\Gamma l}{4 - \Gamma l} \right)^2. \tag{10}$$

Taking finally into account that the threshold condition for the coherent oscillation in a semilinear cavity (Fig. 3C) with reflectivity R of a conventional mirror reads as $RR_{\mathrm{pc}} = 1$, one can obtain for the threshold coupling strength

$$(\Gamma l)_{\mathrm{th}} = \frac{4}{1 + \sqrt{R}}. \tag{11}$$

Equations (8)–(11) allow photovoltaic field E_{12}^{C} to be calculated from experimental values of η, R_{pc}, or $(\Gamma l)_{\mathrm{th}}$ or directly from Γ [see Eq. (8)]. To evaluate the component of the photovoltaic tensor β_{12}^{C}, one must measure specific photoconductivity κ independently.

3. RECORDING OF THREE-DIMENSIONAL PHASE GRATINGS WITH ORTHOGONALLY POLARIZED LIGHT WAVES

In our experiment a light beam from a frequency-doubled diode-pumped Nd^{3+}:YAG laser (single mode, single frequency, $\lambda = 0.53$ μm, 100-mW output power) was used for anisotropic grating recording. A 1-mm-thick $LiNbO_3$ sample, K243, synthesized at the Department of Physics, Moscow State University, contained 0.74 wt. % of yttrium and 0.06 wt. % of iron. The input–output optically finished sample faces and the z axis were parallel to the domain walls, whereas the x axis was normal to the domain walls. The domain structure period was approximately 8 μm.

Owing to the special features of the growth technique used,[9] the sample is inhomogeneous: It contains two peripheral PPLN areas separated by a nearly 3-mm-wide single-domain area. This structure allows for comparison of the results obtained with PPLN and single-domain crystals of identical compositions and dimensions.

Two recording beams (obtained from an unexpanded 1-mm-waist laser beam) impinge symmetrically at an angle $\pm\theta_0$ upon the sample in the XY plane (Fig. 1). The diffraction efficiency is measured at saturation, with only one of two recording waves incident upon the sample and the other one blocked. It is calculated as the ratio of diffracted intensity component I_d to total intensity $I_t + I_d$ transmitted through the sample:

$$\eta = \frac{I_d}{I_d + I_t}. \tag{12}$$

Intensity gain factor $\tilde{\Gamma}$ is calculated from the standard relation

$$\tilde{\Gamma} = \frac{1}{l} \ln \left[\frac{I_e(l)}{I_e(0)} \frac{I_o(0)}{I_o(l)} \right]. \tag{13}$$

For sufficiently small and large input beam ratios we indeed have $\tilde{\Gamma} = \Gamma$.

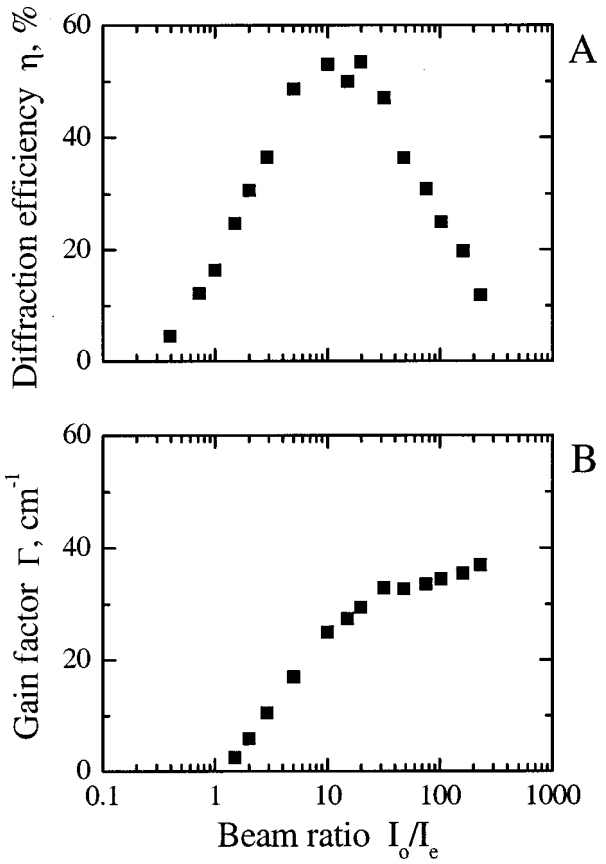

Fig. 4. Dependence on pump ratio of A, diffraction efficiency and B, the two-beam coupling gain factor.

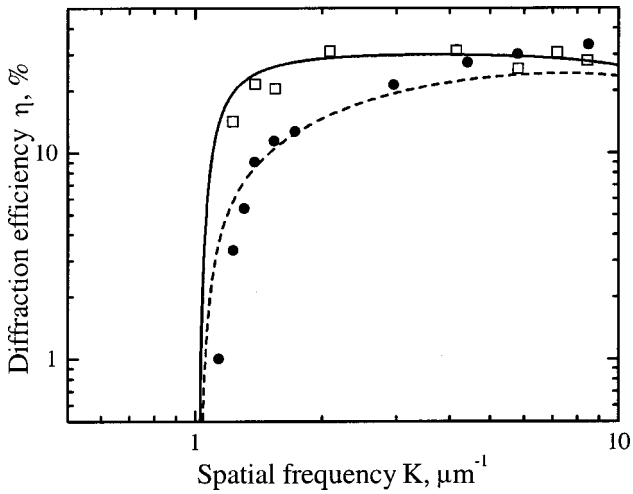

Fig. 5. Measured diffraction efficiency versus spatial frequency for polarization grating recording. Open squares and filled circles, single-domain and PPLN areas, respectively. Solid and dashed curves, theoretical dependences (see text).

Figure 4 shows the dependences $\eta(m)$ (Fig. 4A) and $\tilde{\Gamma}(m)$ (Fig. 4B) on beam ratio for a grating recorded in the PPLN area of the sample. Note the rather high values of the diffraction efficiency (~60%) for the polarization recording and also the difference of the optimum (for η) pump ratio m from unity; the latter feature is typical of media with nonlocal nonlinear response. The small-

signal gain factor ($\tilde{\Gamma} \approx \Gamma$) for *e*-waves approaches 40 cm^{-1}. It should be mentioned also that for beam ratio $m \leqslant 20$ we observe rather strong light-induced scattering, both parametric[6] and wide-angular. This competing nonlinear effect strongly depletes the *e*-waves and reduces the measured values of Γ.

The spatial-frequency dependences of η for the single-domain and PPLN areas of the sample are illustrated in Fig. 5. Equal pump intensities ($m = 1$) are used in this experiment. The solid and dashed curves show the corresponding dependences calculated from Eq. (8) and expression (5) for $2x_0 = \infty$ and $2x_0 = 8\ \mu$m, respectively. The maximum attainable value of the space-charge field is ~7.5 kV/cm for this fit.

4. COHERENT OPTICAL OSCILLATION

A photorefractive crystal pumped by two counterpropagating waves can serve as a phase-conjugate mirror (see, e.g., Ref. 15). With reflectivity R_{pc} larger than 100% (the amplified phase-conjugate reflectivity), this mirror can form (together with a conventional mirror) a cavity (see Fig. 3C) in which coherent oscillation occurs.[16]

The experimental arrangement used for the study of self-oscillation in this semilinear cavity[15] is depicted in Fig. 6. Note that this type of oscillator (with a phase-conjugate mirror) is important because of its ability to compensate for intracavity phase distortions.[15,17]

Coherent oscillation with bulk homogeneously poled $LiNbO_3$:Fe has been known for a long time.[18–20] Unfortunately, the angular divergence of the oscillation wave here is a few orders of magnitude larger than the diffraction limit (of the order of a few degrees[19]) because of strong optical damage.

We have repeated these experiments, using PPLN:Y:Fe instead of bulk iron-doped lithium niobate. The same Nd^{3+}:YAG laser is used to form two *o*-polarized pump waves. The optical (and also polar) axis of the sample is perpendicular to the pump plane; see Fig. 6. The spontaneously arising oscillation waves are *e* polarized. The distance between the sample and mirror M's is 5 cm. With the diameter of the pumped area inside the sample ~1 mm, the Fresnel number of the cavity is ≈20. The

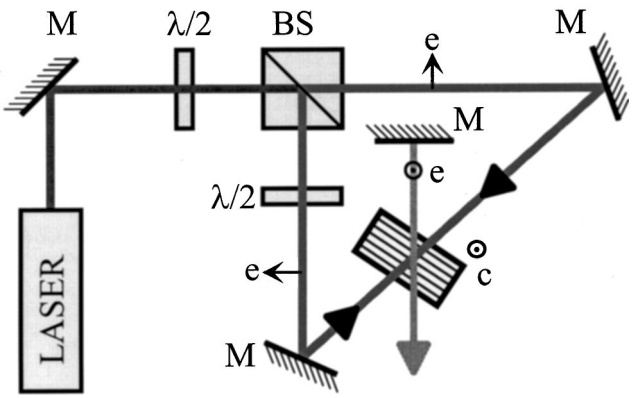

Fig. 6. Experimental arrangement for the study of coherent oscillation in PPLN: M's, flat mirrors; λ/2's, phase retarders; BS, beam splitter.

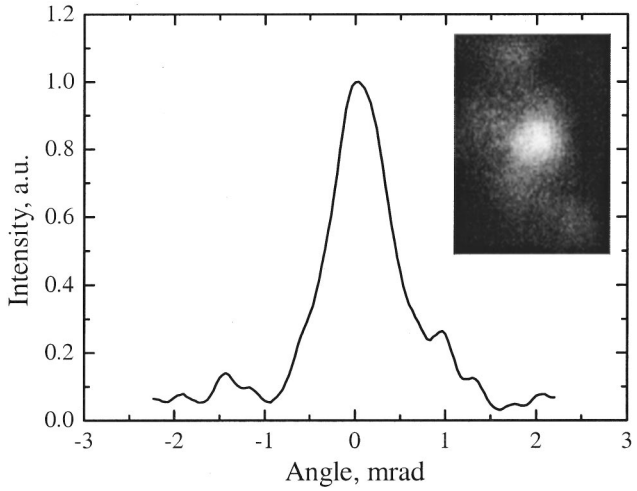

Fig. 7. Far-field light pattern recorded with a CCD-camera (inset) and the corresponding intensity distribution for the oscillation wave. The length of the semilinear cavity is 5 cm; the cavity axis makes an angle of 20° with the pump direction.

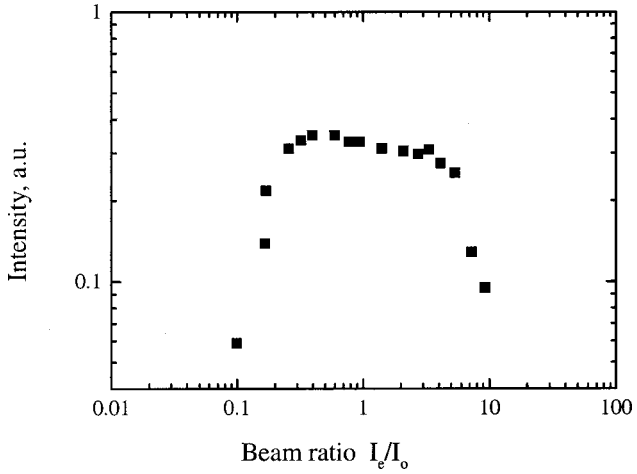

Fig. 8. Oscillation intensity versus beam ratio.

angle between the cavity axis and the pump direction is ≈20°; i.e., the fundamental grating spacing is $\Lambda = 2\pi/K \simeq 1.6\ \mu$m.

Under the conditions described, our 1-mm-thick PPLN sample exhibits well-developed coherent oscillation. It is not possible, however, to achieve self-oscillation with *e*-polarized pump beams because of the unfavorable ($o \rightarrow e$) direction of the nonlinear energy exchange between the crystal eigenmodes; a similar situation takes place in the single-domain case.[12]

Figure 7 shows the far-field pattern of output radiation for our coherent oscillator recorded with a CCD camera (inset) and the intensity distribution in its cross section. The angular divergence (FWHM) here is $\sim 10^{-3}$ rad, i.e., at least 1 order of magnitude smaller than that reported earlier for single-domain crystals.[19]

As distinct from the coherent oscillators based on diffusion photorefractive nonlinearity, the largest output intensity in our case is obtained at equal pump intensities (Fig. 8). The oscillation disappears abruptly for $m \leqslant 0.1$ and $m \geqslant 10$; i.e., the oscillation threshold is highly pronounced.

5. DISCUSSION AND EVALUATION OF PHOTOVOLTAIC PARAMETERS

Our experimental results show that PPLN:Y:Fe is a material that is appropriate for photorefractive recording with two orthogonally polarized crystal eigenwaves, an ordinary wave and an extraordinary wave. Even with a relatively thin sample, $l = 0.1\,\mathrm{cm}$, diffraction efficiency $\eta \approx 60\%$ and coupling strength $\Gamma l \approx 4$ are achieved.

The direct estimate $\Gamma l \approx 3.7\,\mathrm{cm}^{-1}$ from the data of Fig. 4B fits well the values extracted from our measurements of the diffraction efficiency. By setting η=0.57 and $m = 12$ in Eq. (9), we obtain easily $\Gamma l = 4$. One more independent estimate of the product Γl can be obtained from the position of the maximum of the dependence $\eta(m)$. As follows from Eq. (9), the largest diffraction efficiency has to be reached at the beam ratio

$$m^{\max} = \exp\left(-\frac{\Gamma l}{2}\right). \tag{14}$$

Using the experimental value $m^{\max} = 12$ (Fig. 4B), we have $\Gamma l = 5$, which is not far from the direct estimate made above.

With the gain factor known, we can evaluate the photovoltaic field. Using Eq. (8) and the values $n = 2.3$, $r_{51} = 28 \times 10^{-10}\,\mathrm{cm/V}$, and λ=0.53 μm, we have $E_{12}^{C} = \beta_{12}^{C}/\kappa \approx 7.5\,\mathrm{kV/cm}$. This value is compatible with the data known for the single-domain $LiNbO_3$:Fe crystals. We can conclude therefore that the presence of yttrium does not much (if at all) influence the photovoltaic properties of iron-doped PPLN samples.

The photovoltaic parameters can also be evaluated from the characteristics of the coherent oscillation. The presence of this threshold phenomenon proves unambiguously that our PPLN sample ensures the amplified phase-conjugate reflectivity, $R_{\mathrm{pc}} > 100\%$. This result might be surprising at first glance because the diffraction efficiency of a grating recorded with the optimized beam ratio does not exceed 60%. However, there is no contradiction here because we are dealing with a rather specific (in-phase) superposition of two photorefractive gratings, each recorded by two copropagating waves. The initial grating recorded by the signal wave together with the copropagating pump wave is coherently enhanced by the grating recorded with the other pump wave and the generated phase-conjugate wave. This results in the highest possible efficiency of phase conjugation by means of backward four-wave mixing. Note that in classic $\chi^{(3)}$ media these two gratings are mutually shifted by $\pi/2$ and in crystals with gradient photorefractive nonlinearity they are exactly out of phase (mutually shifted by π). Consequently the net phase-conjugate reflectivity is smaller (at the same coupling strength) for these nonlinearities than for the nonlinearity caused by the circular photovoltaic effect. To attain values $R_{\mathrm{pc}} > 1$ the product Γl should be at least larger than 2, as follows from Eq. (10), which indeed does not contradict our previous estimates.

The value of Γl can also be extracted from the experimental data on the threshold pump ratio. The relevant threshold condition is known from the theory of polarization four-wave coupling.[14] For the case under study ($|E_{12}^{C}| \gg |E_{15}^{L}|$) we have

$$R_{\mathrm{pc}} = \frac{1 - \Delta^2}{[1 - \Delta \tanh(\Gamma l \Delta/4)]^2}, \tag{15}$$

where $\Delta = (m - 1)/(m + 1)$. With $m_{\mathrm{th}} = 0.1$ we arrive at coupling strength $\Gamma l \approx 3$. This value is somewhat smaller than that extracted from two-beam coupling experiments, most probably because of cavity losses such as from Fresnel reflections from the crystal face and crystal absorption. This estimate in fact gives only the lowest limit for the threshold coupling strength.

It should be noted that with Γl approaching 4 the oscillator considered is still below the threshold of coherent mirrorless oscillation predicted in Ref. 12 and experimentally observed in bulk homogeneously poled crystals.[21]

6. CONCLUSIONS

Periodically poled lithium niobate codoped with iron and yttrium possesses almost the same photorefractive sensitivity to polarization grating recording as that of bulk homogeneously poled crystals. This means that even a large amount of yttrium in the samples does not strongly reduce the photorefractive nonlinearity related to the iron centers.

Highly efficient frequency-degenerate wave mixing is possible with PPLN:Y:Fe in classic backward-wave geometry (phase conjugation, various photorefractive oscillators) as well as in forward-wave geometry (parametric amplification of copropagating coherent seed waves).

By varying domain size x_0 it is possible to control the cutoff spatial frequency[4,5,22,23] below which the photorefractive sensitivity of periodically poled material decreases. This control can be accomplished with periodically poled lithium niobate, but the technique can be especially effective for crystals with low birefringence, such as periodically poled lithium tantalite.

ACKNOWLEDGMENTS

We are grateful to I. Naumova for furnishing PPLN samples. Partial financial support from the U.S. Civilian Research and Development Foundation in Ukraine (grant UP2-2122) is gratefully acknowledged.

REFERENCES

1. J. A. Armstrong, N. Bloembergen, J. Ducuing, and P. S. Pershan, "Interaction between light waves in a nonlinear dielectric," Phys. Rev. **127**, 1918–1939 (1962).
2. R. L. Byer, "Quasi-phasematched nonlinear interactions and devices," J. Nonlinear Opt. Phys. Mater. **6**, 549–592 (1997).
3. G. Rosenman, A. Skliar, and A. Arie, "Ferroelectric domain engineering for quasi-phase-matched nonlinear optical devices," Ferroelectr. Rev. **1**, 263–326 (1999).
4. B. Sturman, M. Aguilar, F. Agulló-Lopez, V. Pruneri, and P. G. Kazansky, "Photorefractive nonlinearity of periodically poled ferroelectrics," J. Opt. Soc. Am. B **14**, 2641–2649 (1997).
5. S. Odoulov, T. Tarabrova, A. Shumelyuk, I. I. Naumova, and T. O. Chaplina, "Photorefractive response of bulk periodically poled $LiNbO_3$:Y:Fe at high and low spatial frequencies," Phys. Rev. Lett. **84**, 3294–3297 (2000).

6. M. Goulkov, S. Odoulov, I. Naumova, F. Agulló-Lopez, G. Calvo, E. Podivilov, B. Sturman, and V. Pruneri, "Degenerate parametric light scattering in periodically poled $LiNbO_3$:Y:Fe," Phys. Rev. Lett. **86**, 4021–4024 (2001).
7. B. I. Sturman and V. M. Fridkin, *Photovoltaic and Photorefractive Effects in Noncentrosymmetric Materials* (Gordon & Breach, Philadelphia, Pa., 1992).
8. S. Odoulov, "Spatially oscillating photovoltaic current in iron-doped lithium niobate crystals," JETP Lett. **35**, 10–13 (1982).
9. N. F. Evlanova, I. I. Naumova, T. O. Chaplina, S. A. Blokhin, and S. V. Lavrischev, "Periodically poled Y:$NiNbO_3$ single crystal: impurity distribution and domain wall location," J. Cryst. Growth **223**, 156–160 (2001).
10. S. Odoulov, "Vectorial interactions in photovoltaic media," Ferroelectrics **91**, 213–225 (1989).
11. E. V. Podivilov, B. I. Sturman, M. Goulkov, S. Odoulov, G. Calvo, F. Agulló-López, and M. Carrascosa, "Parametric scattering processes in photorefractive PPLN," J. Opt. Soc. Am. B **19**, 1582–1591 (2002).
12. A. Novikov, S. Odoulov, O. Oleinik, and B. Sturman, "Beam-coupling, four-wave mixing and optical oscillation due to spatially-oscillating photovoltaic currents in lithium niobate crystals," Ferroelectrics **75**, 295–315 (1987).
13. N. Kukhtarev, V. Markov, S. Odoulov, M. Soskin, and V. Vinetski, "Holographic storage in electrooptic crystals," Ferroelectrics **22**, 949–964 (1979).
14. A. Novikov, V. Obukhovsky, S. Odoulov, and B. Sturman, "Explosion instability and coherent optical oscillation in photorefractive crystals," Sov. Phys. JETP **44**, 538–542 (1986).
15. M. Cronin-Golomb, B. Fischer, J. O. White, and A. Yariv, "Theory and applications of four-wave mixing in photorefractive media," IEEE J. Quantum Electron. **QE-20**, 12–30 (1984).
16. J. Feinberg and R. Hellwarth, "Phase-conjugating mirror with continuous-wave gain," Opt. Lett. **5**, 519–521 (1980).
17. A. A. Bagan, V. B. Gerasimov, A. V. Golyanov, V. E. Ogluzdin, V. A. Sugrobov, I. L. Rubtsova, and A. I. Khyzhnjak, "Conditions for the stimulated emission from a laser with cavities coupled via a dynamic hologram," Sov. J. Quantum Electron. **17**, 49–52 (1990).
18. S. Odoulov and M. Soskin, "Lithium niobate laser with frequency-degenerate pumping," JETP Lett. **37**, 289–293 (1983).
19. S. Odoulov, "Self-excitation of lasing in lithium niobate during recording of dynamic phase gratings by circular photogalvanic currents," Sov. J. Quantum Electron. **14**, 360–364 (1984).
20. S. H. Wemple, M. Di Domenico, and J. Camlibel, "Dielectric and optical properties of melt-grown $BaTiO_3$," J. Phys. Chem. Solids **29**, 1797–1803 (1968).
21. S. Odoulov, R. Jungen, and T. Tschudi, "Mirrorless oscillation due to vectorial four-wave mixing in $LiNbO_3$:Fe," Appl. Phys. B **56**, 57–61 (1993).
22. M. Taya, M. C. Bashew, and M. M. Fejer, "Photorefractive effects in periodically poled ferroelectrics," Opt. Lett. **21**, 857–859 (1996).
23. S. Odoulov and B. Sturman, "Photorefraction with the photovoltaic charge transport," in *Progress in Photorefractive Nonlinear Optics*, K. Kuroda, ed., Proceedings of the Waseda Symposium (Francis & Taylor, Tokyo, 2001), pp. 113–132.